Electronic Supplementary Material (ESI) for Dalton Transactions.

Perovskite Alkali Metal Samarium Borohydrides: Crystal Structures and Thermal Decomposition

Kasper T. Møller,[1] Alexander S. Fogh,[1] Mathias Jørgensen,[1] Torben R. Jensen[1*]

[1]*Interdisciplinary Nanoscience Center (iNANO) and Department of Chemistry, University of Aarhus, DK-8000 Aarhus, Denmark*

*Corresponding Author
Torben R. Jensen, trj@chem.au.dk

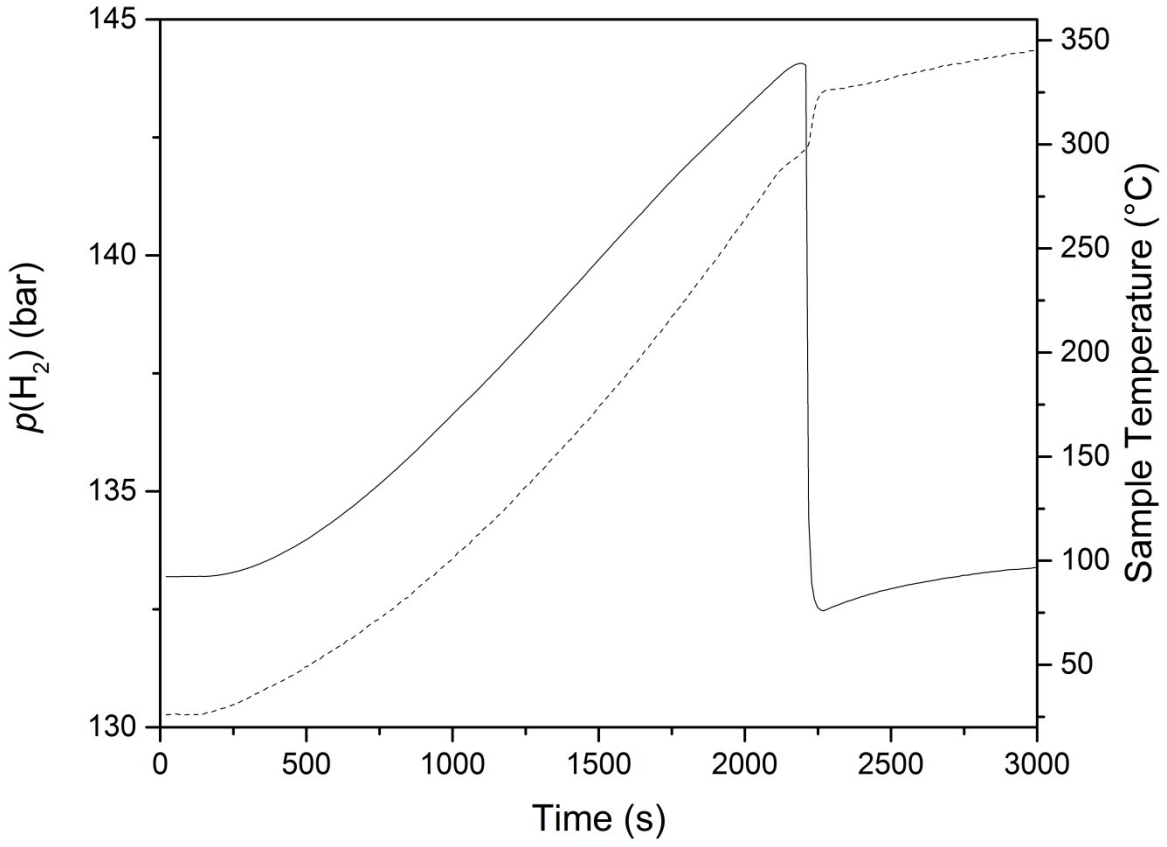

Figure S1. The hydrogen absorption of Sm metal to form SmH_2. The dashed line indicates the temperature while the solid line indicates the hydrogen pressure.

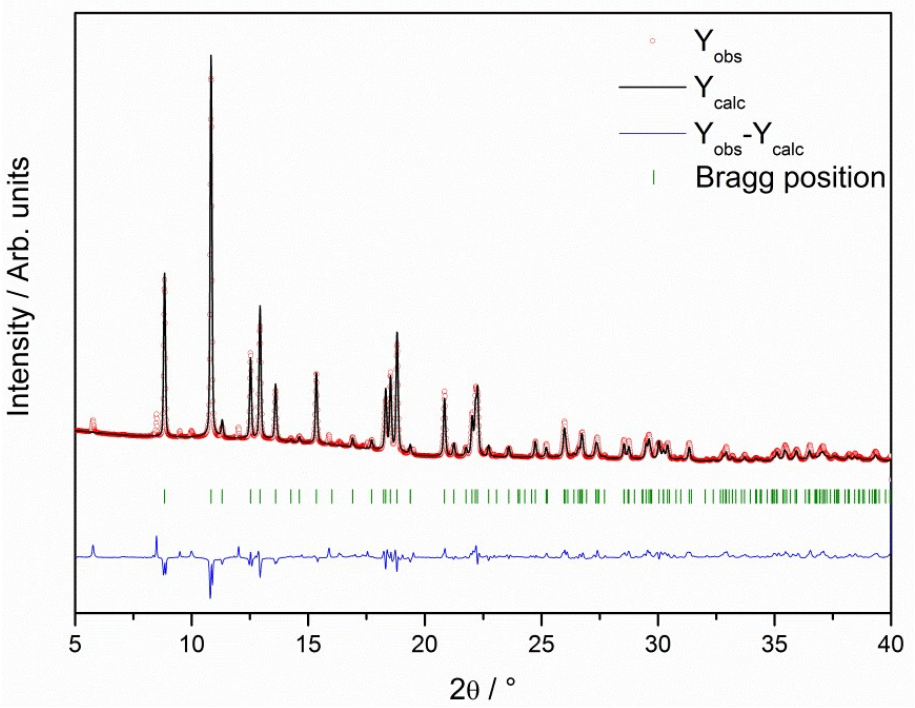

Figure S2. Rietveld refinement of the SR-PXD of $Sm(BH_4)_2$ synthesized from SmH_2 in $THF{\cdot}BH_3$ (λ = 0.8212 Å). $Sm(BH_4)_2$: green marker, observed data (Y_{obs}, red curve), Rietveld refinement profile (Y_{calc}, black curve), and difference plot ($Y_{obs} - Y_{calc}$, blue curve). Extracted unit cell parameters: a = 6.9349(3) Å, b = 8.3339(4) Å and c = 7.5279(3) Å. Space-group: *Pbcn*. R_{Bragg} = 15.5%.

Samarium(II) borohydride, $Sm(BH_4)_2$, is identified in the sample by SR-PXD. A structural model published elsewhere,[1] was applied for Rietveld refinement and is in accord with the observed data. However, a set of unidentified reflections are also observed, which may be associated with a solvate.

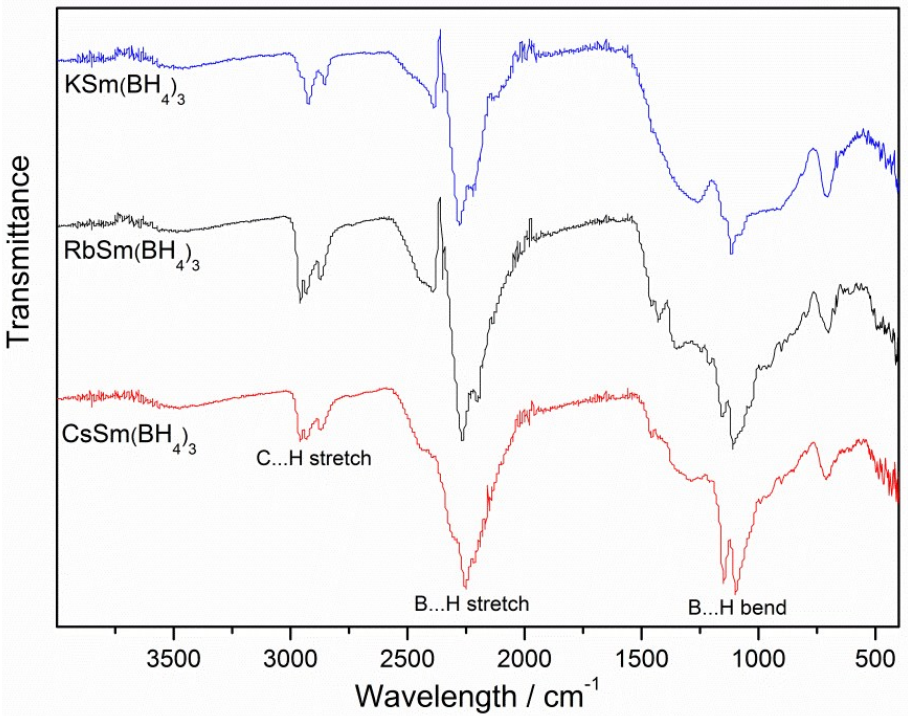

Figure S3. FT-IR on annealed samples of MSm$(BH_4)_3$, M = K, Rb, Cs.

FT-IR of the annealed MSm$(BH_4)_3$ samples indicates B–H bending and stretching modes at 2300-2200 and 1350-1100 cm^{-1}, respectively. However, characteristic C–H stretches are also observed at 2960-2850 cm^{-1}, possibly from remaining solvent.

Volume per formula unit (V/Z) Calculations

$KSm(BH_4)_3$:

$\sum V(KBH_4)+V(Sm(BH_4)_2) = 749.67$ Å^3

V(KSm(BH4)3) = 744.26 Å^3

Z = 4

$\Delta(V/Z) = (5.41/4)$ Å^3 = - 1.35 Å^3

Hence, 1.35 Å^3/(749.67 Å^3/4) = 0.72 % smaller.

$RbSm(BH_4)_3$:

$\sum V(RbBH_4)+V(Sm(BH_4)_2) = 792.51$ Å^3

V(RbSm(BH4)3) = 782.3 Å^3

Z = 4

$\Delta(V/Z) = (10.21/4)$ Å^3 = 2.55 Å^3

Hence, 2.55 Å^3/(792.51 Å^3/4) = 1.29 % smaller.

$CsSm(BH_4)_3$:

$\sum V(CsBH_4)+V(Sm(BH_4)_2) = 853.58$ Å^3

Z = 4

V/Z = 213.3395 Å^3

V(CsSm(BH4)3) = 406.35 Å^3

Z = 2

V/Z = 203.18 Å^3

$\Delta(V/Z) = 10.215$ Å^3

Hence, 10.215 Å^3/213.3395 Å3 = 4.79 % smaller.

The small deviation of $KSm(BH_4)_3$ is similar to $KZn(BH_4)Cl_2$ ($\Delta(V/Z)$ = 0.66 %),[2] which is also formed by ball-milling. Addtionally, $LiK(BH_4)_2$ has a $\Delta(V/Z)$ = 5.53 % and is also formed by ball-milling.[3] Hence, the thermal requirement for formation of $RbSm(BH_4)_3$ and $CsSm(BH_4)_3$ is unexpected, and usually only observed in compounds where $\Delta(V/Z)$ deviates positively.[4]

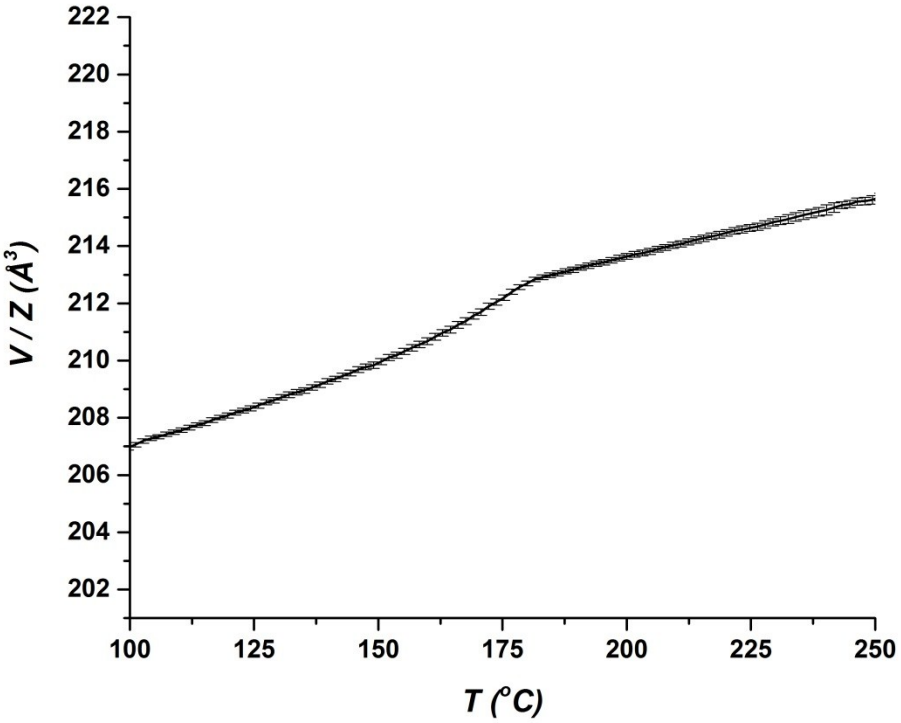

Figure S4. Increase in unit cell volume of $CsSm(BH_4)_3$ as function of temperature.

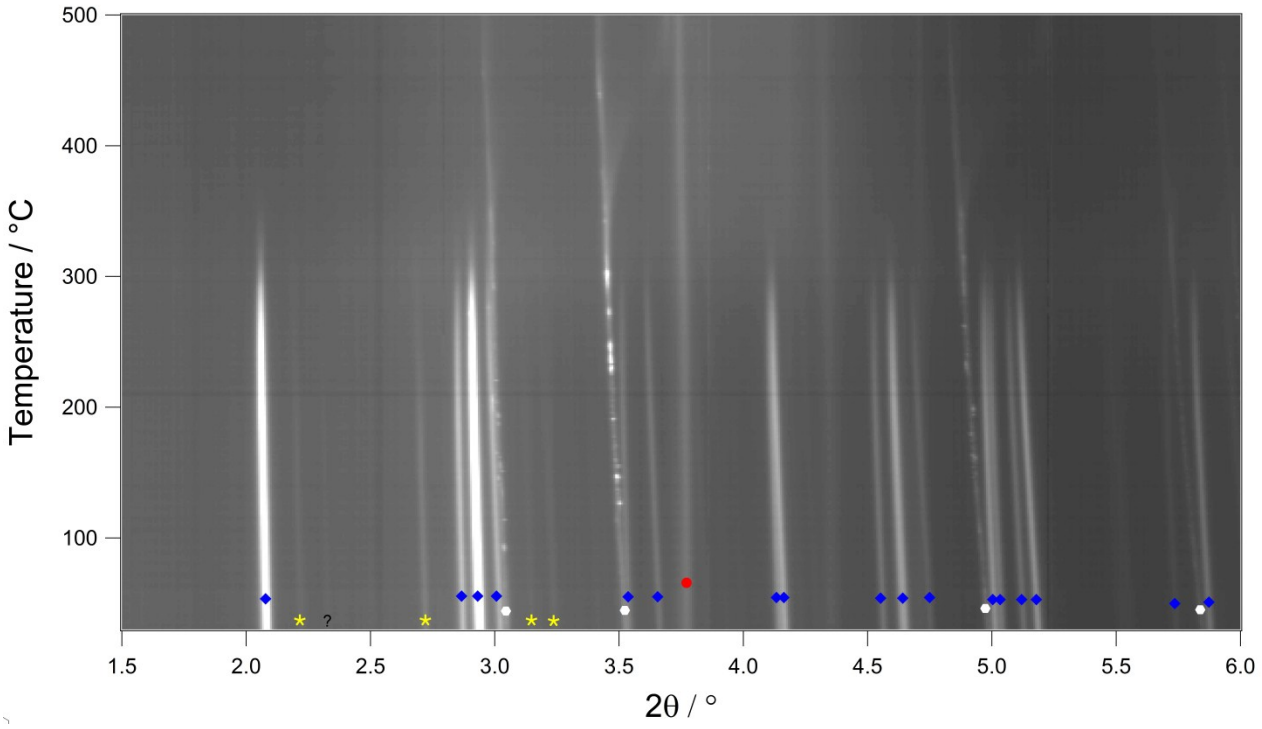

Figure S5. *In situ* SR-PXD data of the annealed $KSm(BH_4)_3$ sample measured from *RT* to 500 °C, $\Delta T/\Delta t$ = 10 °C min^{-1} at *p*(Ar) = 1 bar (λ = 0.2072 Å). Symbols: $Sm(BH_4)_2$ (yellow star), $KSm(BH_4)_3$ (blue diamond), KBH_4 (white hexagon), Sm_2O_3 (red circle), Unknown (black question mark).

Initially, the SR-PXD data show the reactants, KBH_4 and $Sm(BH_4)_2$, the product, $KSm(BH_4)_3$ and small fractions of Sm_2O_3 and an unidentified impurity. Bragg reflections from $Sm(BH_4)_2$ disappear at $T \sim 330$ °C which is similar reported decomposition temperature.[1] Soon after, $KSm(BH_4)_3$ decompose at $T \sim 345$ °C which is very similar to the observation made in the *in situ* experiment for the as-milled KBH_4–$Sm(BH_4)_2$ (1:1) sample.

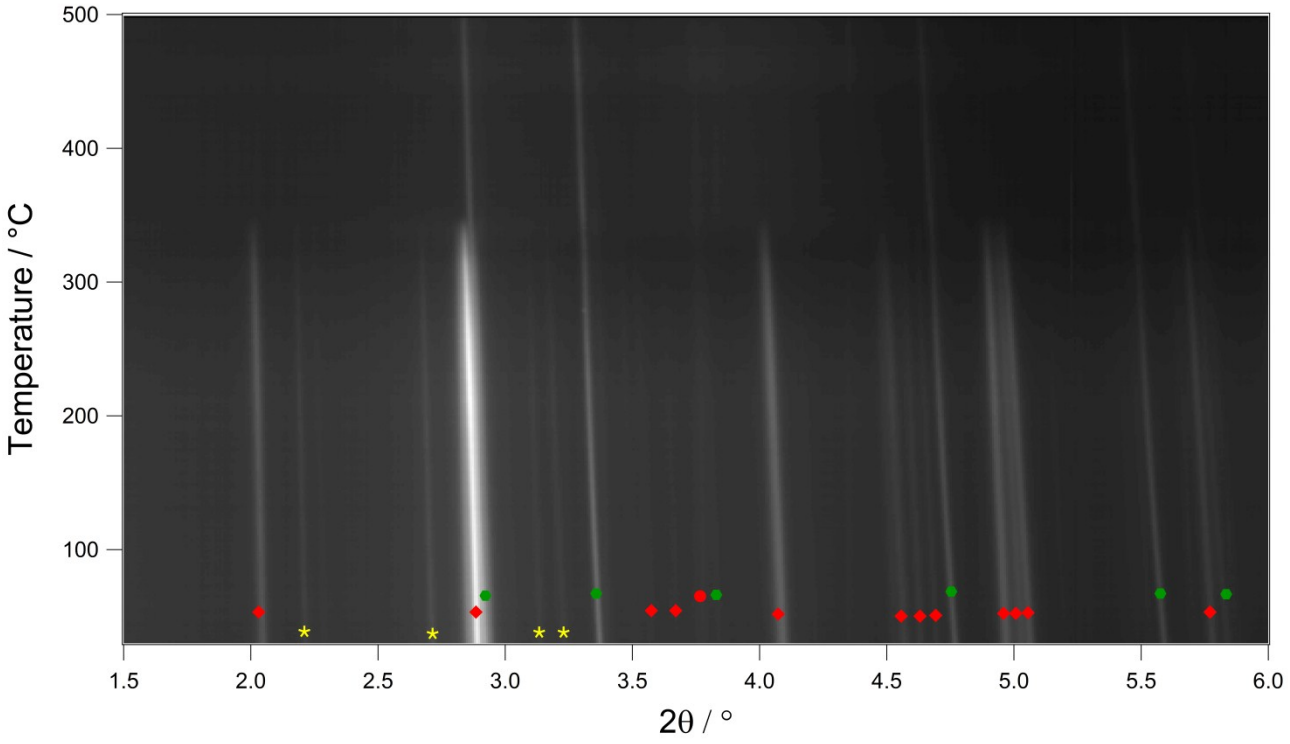

Figure S6. *In situ* SR-PXD data of the annealed $RbSm(BH_4)_3$ sample measured from *RT* to 500 °C ($\Delta T/\Delta t$ = 10 °C min^{-1}) at p(Ar) = 1 bar (λ = 0.2072 Å). Symbols: $Sm(BH_4)_2$ (yellow star), $RbSm(BH_4)_3$ (red diamond), $RbBH_4$ (green hexagon), Sm_2O_3 (red circle).

Initially, the SR-PXD data show the reactants, $RbBH_4$ and $Sm(BH_4)_2$, the product, $RbSm(BH_4)_3$ and a small fraction of Sm_2O_3. Bragg reflections from $Sm(BH_4)_2$ and $KSm(BH_4)_3$ disappear at $T \sim 330$ °C and $T \sim 345$ °C, respectively, which is very similar to the observations made in the *in situ* experiments for the as-milled $RbBH_4$–$Sm(BH_4)_2$ (1:1) and the $KSm(BH_4)_3$ sample.

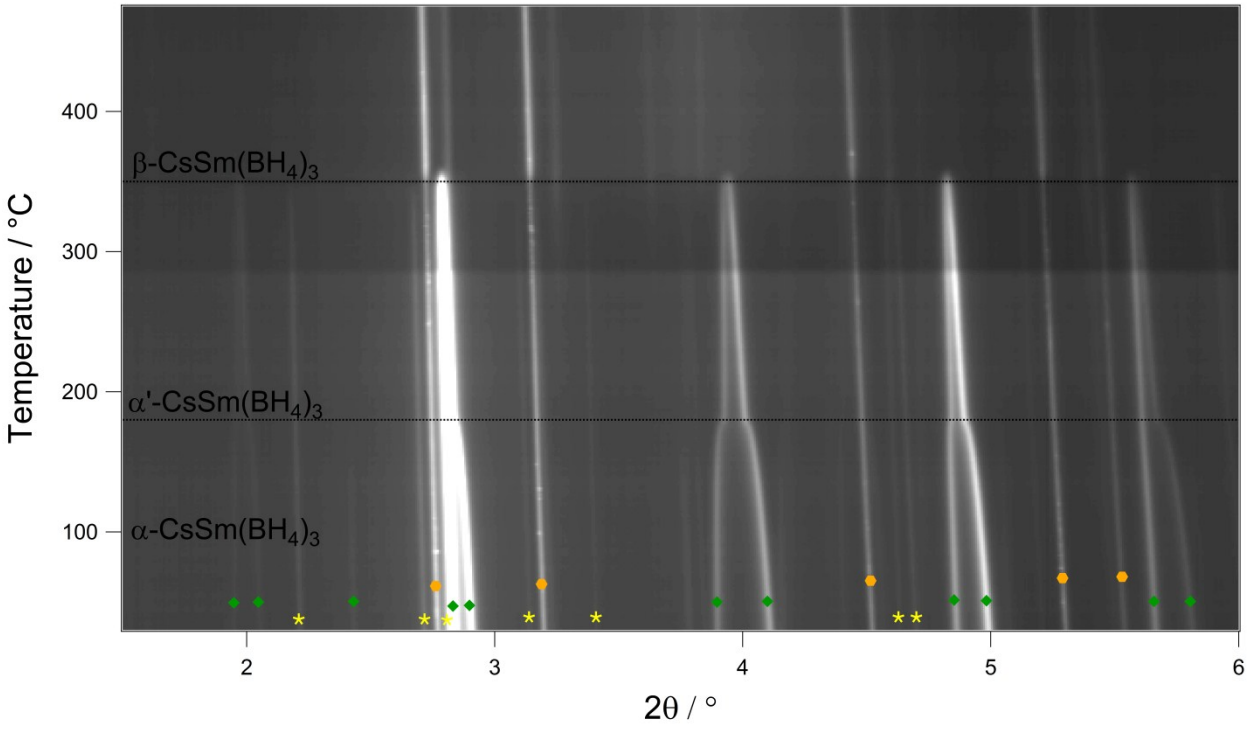

Figure S7. *In situ* SR-PXD data of the annealed $CsSm(BH_4)_3$ sample measured from *RT* to 475 °C ($\Delta T/\Delta t$ = 10 °C min^{-1}) at *p*(Ar) = 1 bar (λ = 0.2072 Å). Symbols: $Sm(BH_4)_2$ (yellow star), $CsSm(BH_4)_3$ (green diamond), $CsBH_4$ (orange hexagon).

Initially, the SR-PXD data show the reactants, $CsBH_4$ and $Sm(BH_4)_2$, and the product, $CsSm(BH_4)_3$. In the temperature range *RT* to ~ 358 °C, Bragg reflections at 2θ ~ 2.9, 3.90, 4.11, 4.86, 4.99 and 5.82° (*d* ~ 4.08, 3.05, 2.89, 2.44, 2.38 and 2.04 Å) approaches existing reflections and eventually merge together in the second-order polymorphic transition. Bragg reflections from $Sm(BH_4)_2$ and $KSm(BH_4)_3$ disappear at *T* ~ 338 °C and *T* ~ 360 °C, respectively.

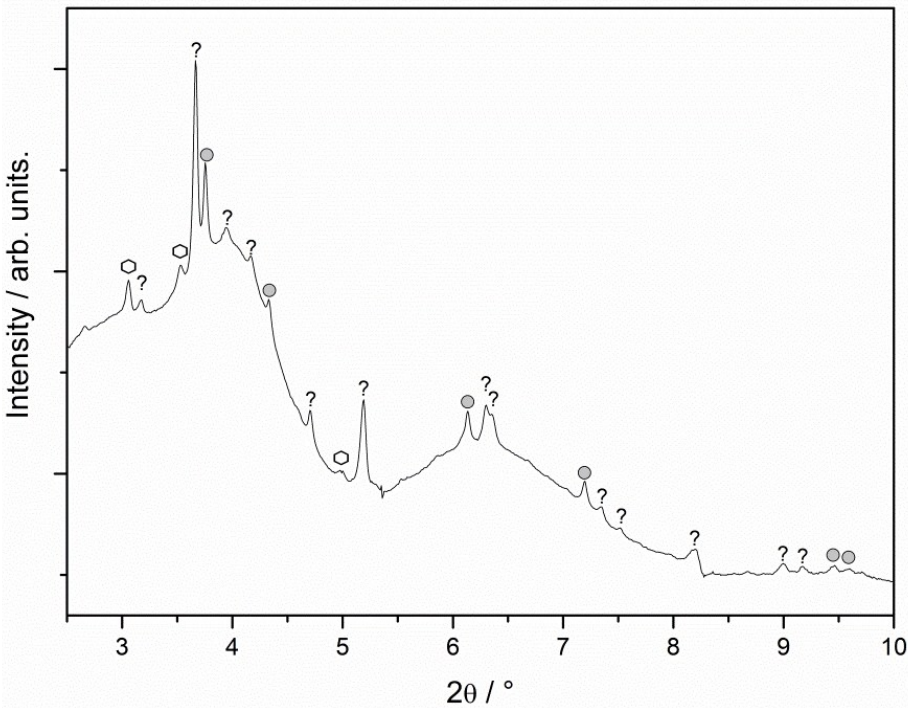

Figure S8. SR-PXD of the decomposition products of the $KSm(BH_4)_3$ (λ = 0.2072 Å) sample. Symbols: white hexagon: $RbBH_4$; grey circle: SmH_2; black question mark: Unknown.

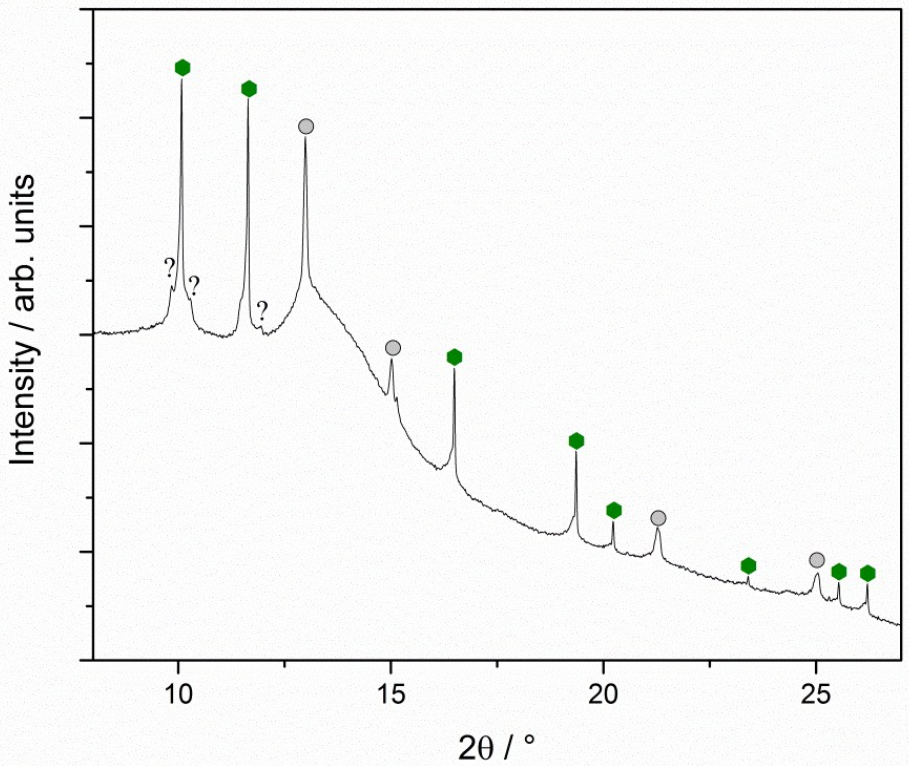

Figure S9. SR-PXD of the decomposition products of the $RbSm(BH_4)_3$ (1:1, λ = 0.7129 Å) sample. Symbols: green hexagon: $RbBH_4$; grey circle: SmH_2; black question mark: Unknown.

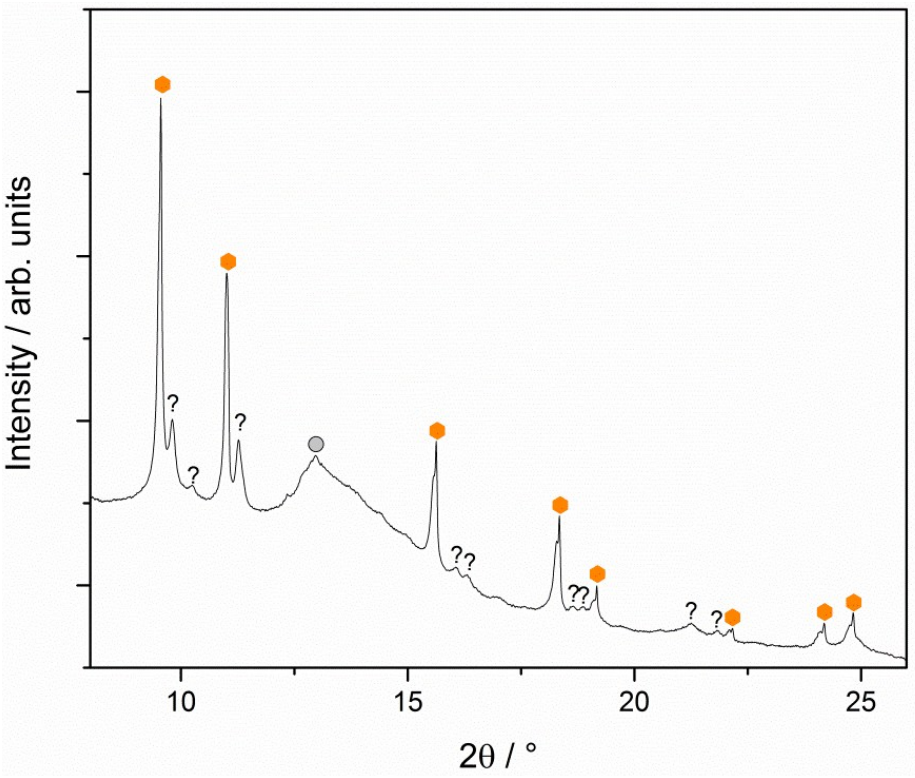

Figure S10. SR-PXD of the decomposition products of the $CsSm(BH_4)_3$ (λ = 0.7129 Å) sample. Symbols: orange hexagon: $CsBH_4$; grey circle: SmH_2; black question mark: Unknown.

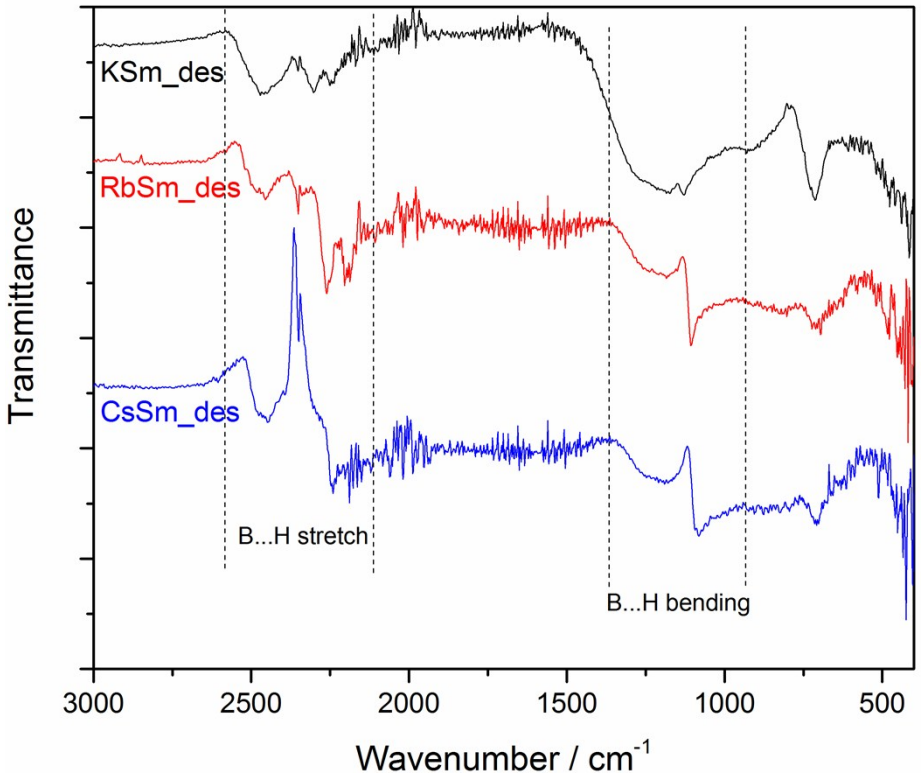

Figure S11. FT-IR on the desorbed samples of MSm$(BH_4)_3$, M = K, Rb, Cs.

FT-IR of the desorped MSm$(BH_4)_3$ samples shows B–H bending modes at 2500-2450 cm^{-1} which may indicate a higher borane species *e.g.* $SmB_{12}H_{12}$. Additional B–H bending and stretching modes are present at 2260-2180 and 1130-1080 cm^{-1} which belong to the respective $M$$BH_4$.

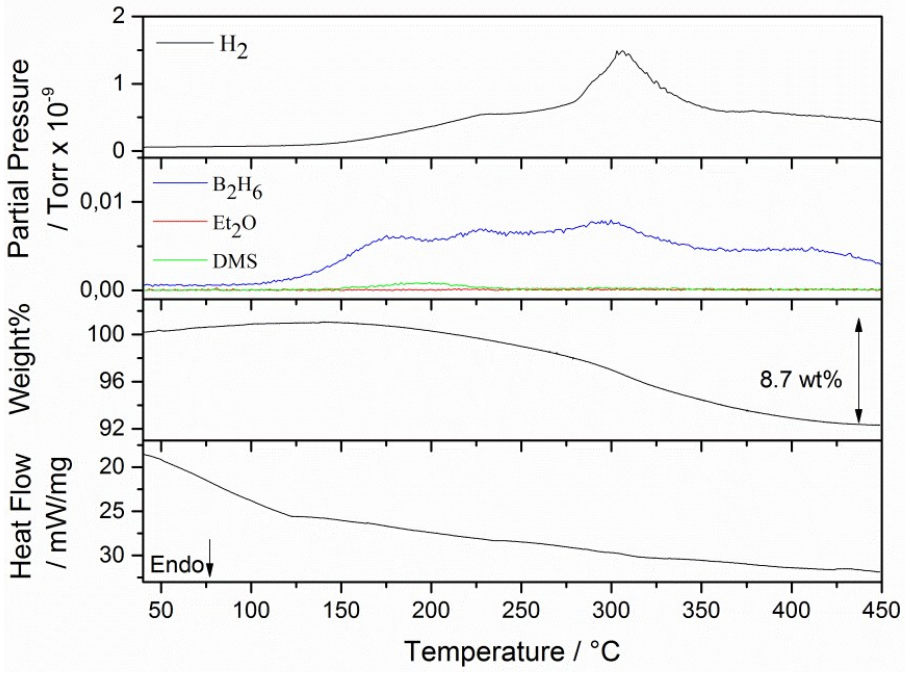

Figure S12. Differential scanning calorimetry (bottom), thermogravimetric analysis (second from bottom) and mass spectrometry (two top ones) data measured from *RT* to 450 °C of $KSm(BH_4)_3$ ($\Delta T/\Delta t$ = 3 °C min^{-1}, Ar flow). Mass spectrometry (two top ones) shows hydrogen (m/z = 2) and diborane, B_2H_6 (m/z = 28).

Thermal analysis of the $KSm(BH_4)_3$, Figure S11, shows an endothermic DSC event at T = 120 °C which is associated with the initiating diborane release at T = 105 °C observed in MS. The diborane release has three peak temperatures at T = 175, 225 and 300 °C. A minor hydrogen release initiates at T = 130 °C with peak temperature at T = 230. At T = 280 °C a major hydrogen release initiates, which peaks at T = 306 °C. Another endothermic event is observed at T = 315 °C, which is slightly higher in temperature than the major release of hydrogen and the peak of diborane. The total weight release over the temperature range amounts to 8.7 wt%.

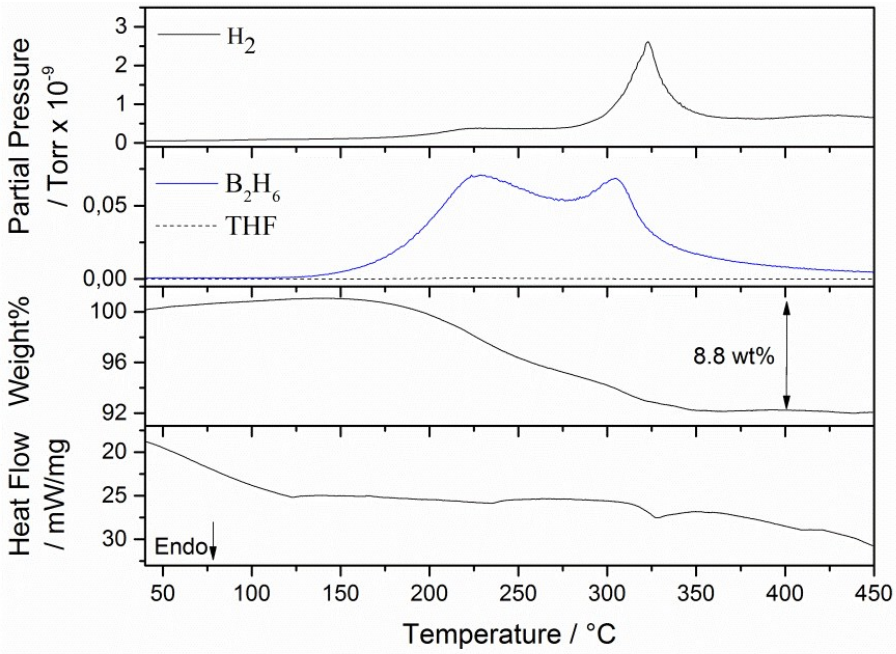

Figure S13. Differential scanning calorimetry (bottom), thermogravimetric analysis (second from bottom) and mass spectrometry (two top ones) data measured from *RT* to 450 °C of $CsSm(BH_4)_3$ ($\Delta T/\Delta t$ = 3 °C min^{-1}, Ar flow). Mass spectrometry (two top ones) shows hydrogen (m/z = 2) and diborane, B_2H_6 (m/z = 28).

Thermal analysis of the $CsSm(BH_4)_3$, Figure S12, shows an endothermic DSC event at T = 123 °C which is associated with the initiating diborane release at T = 125 °C observed in MS. A second endothermic event is observed at T = 235 °C. This event is associated with a small peak in hydrogen release at T = 223 °C and a major diborane release with peak temperature at T = 227 °C. The diborane release has a second peak temperature at T = 305 °C whilst a major hydrogen release initiates at T = 277 °C and peaks at T = 323 °C. Both gas releases are associated with a third endothermic event observed at T = 328 °C. Finally, a fourth endothermic DSC event is observed at T = 410 °C. The total weight release over the temperature range amounts to 8.8 wt%.

Table S1. Summary of DSC events, mass loss, and MS peak temperatures observed in the synthesised MSm$(BH_4)_3$ (M = K, Rb, Cs) and in Sm$(BH_4)_2$ for comparison.

Compound	DSC [°C]	TG [wt%]	MS(H_2) [°C]	MS(B_2H_6) [°C]	Ref
$KSm(BH_4)_3$	120 (endo) 315 (endo)	8.7	230, 306	175, 225, 300	This study
$RbSm(BH_4)_3$	122 (endo) 234 (endo) 325 (endo) 413 (endo)	15.6	(225), 315	(205), 305	This study
$CsSm(BH_4)_3$	123 (endo) 235 (endo) 328 (endo) 410 (endo)	8.8	223, 323	227, 305	This study
$Sm(BH_4)_2$	230 (endo) 313 (endo)	26 wt%	180, 240, 325	180, 230, 310	[1]

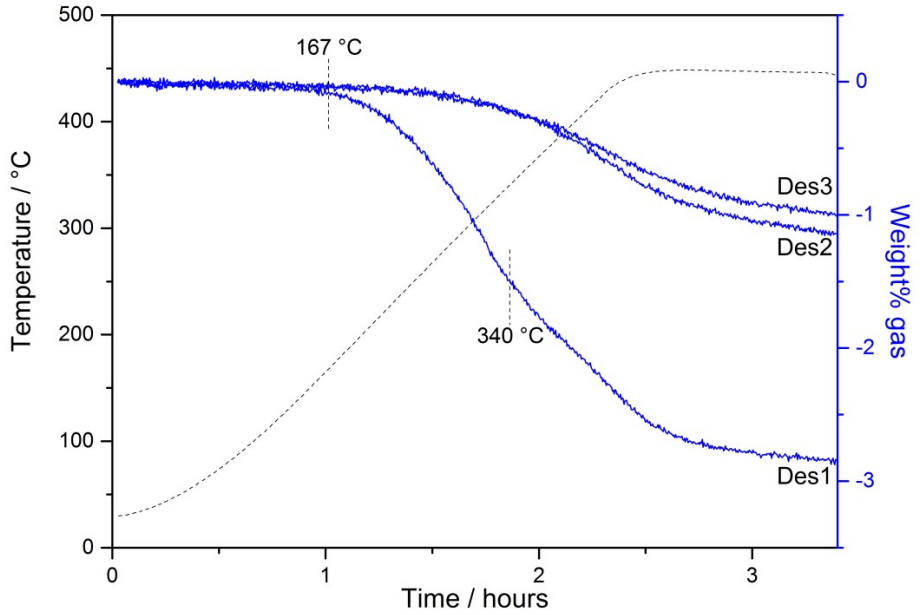

Figure S14. Sieverts measurement of $KSm(BH_4)_3$ showing the three desorption curves conducted in the temperature range *RT* – 450 °C ($\Delta T/\Delta t$ = 3 °C/min, fixed at 450 °C for 1 hour and $p(H_2)$ = 1 bar).

The $KSm(BH_4)_3$ sample shows a continuous gas release which is initiated at $T \sim 167$ °C and continues to $T \sim 340$ °C, see Figure S13. This fits well with the observation in the *in situ* SR-PXD data where $Sm(BH_4)_2$ decrease in intensity and may gradually decompose in this temperature range. The amount of gas released is 1.51 wt%. At $T \sim 340$ °C the gas release rate changes which indicates a second decomposition step. The gas release continues as the temperature reaches 450 °C and eventually amounts to 2.85 wt% H_2 after a 1 hour isotherm at 450 °C. This is slightly lower than the theoretically calculated hydrogen release from $KSm(BH_4)_3$. The second and third desorption curves initiate a gas release at approximately 270 – 280 °C which continues throughout the measurement, ending in a total gas release of 1.1 and 1.0 wt%, respectively.

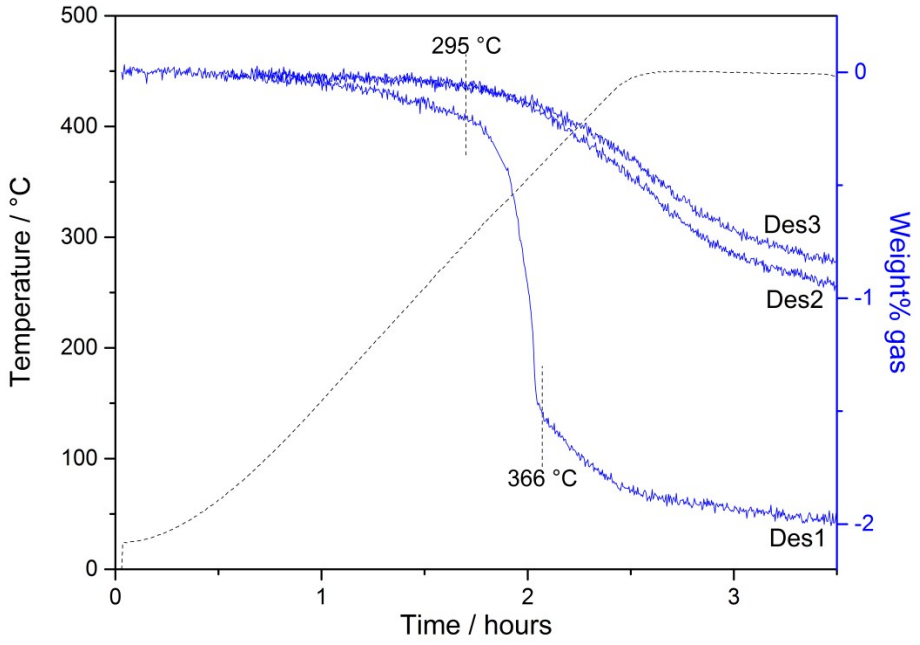

Figure S15. Sieverts measurement of $CsSm(BH_4)_3$ showing the three desorption curves conducted in the temperature range RT – 450 °C ($\Delta T/\Delta t$ = 3 °C/min, fixed at 450 °C for 1 hour and $p(H_2)$ = 1 bar).

The $CsSm(BH_4)_3$ sample shows a continuous gas release of 0.2 wt% in the temperature range *RT* to 295 °C, see Figure S14. At T = 295 °C a significant gas release initiates which continues up to 366 °C and amounts to 1.3 wt%. Another 0.5 wt% is released during a second significant gas release between $T \sim$ 366 to 450 °C which continues during the isothermal conditions. Hence, a total of 2.0 wt% gas is released from the sample, which is slightly more than theoretically possible.

The second and third desorption curve initiates at approximately $T \sim$ 300 °C releasing 0.94 and 0.84 wt%, respectively.

References

1T. D. Humphries, M. B. Ley, C. Frommen, K. Munroe, T. R. Jensen and B. C. Hauback, *J. Mater. Chem. A*, 2014, **3**, 691–698.
2J. Huot, D. B. Ravnsbæk, J. Zhang, F. Cuevas, M. Latroche and T. R. Jensen, *Prog. Mater. Sci.*, 2013, **58**, 30–75.
3 M. B. Ley, E. Roedern and T. R. Jensen, *Phys Chem Chem Phys*, 2014, **16**, 24194–24199.
4 S. R. H. Jensen, L. H. Jepsen, J. Skibsted and T. R. Jensen, *J. Phys. Chem. C*, 2015, **119**, 27919–27929.